Environ. Sci. Technol. **2000**, *34*, 62−70

Colloid Transport and Filtration of *Cryptosporidium parvum* in Sandy Soils and Aquifer Sediments

THOMAS HARTER* AND SONJA WAGNER†

Department of Land, Air, and Water Resources, University of California at Davis, 9240 South Riverbend Avenue, Parlier, California 93648

EDWARD R. ATWILL

Veterinary Medicine Teaching and Research Center, School of Veterinary Medicine, University of California at Davis, 18830 Road 112, Tulare, California 93274

We present theoretical and experimental work on *Cryptosporidium parvum* oocysts to characterize their transport behavior in saturated, sandy sediments under strictly controlled conditions. Column experiments are implemented with three different sands (effective grain size: 180, 420, and 1400 μm) at two different saturated flow rates (0.7 and 7 m/d). The experiments show that *C. parvum* oocysts, like other colloids, are subject to velocity enhancement. In medium and coarse sands, the oocysts travel 10−30% faster than a conservative tracer. The classic clean-bed filtration model is found to provide an excellent tool to estimate the degree of *C. parvum* filtration. Experimentally determined collision efficiencies, α, range from 0.4 to 1.1. The magnitude of α is consistent with the known physical and chemical properties of the oocyst and the transport medium and compares well with, e.g., measured collision efficiencies of similarly sized *E. coli* bacteria. However, a significant amount of the initial deposition appears to be reversible leading to significant asymmetry and tailing in the oocyst concentration breakthrough curve. We are able to show that the observed late-time oocyst elution can qualitatively be explained by postulating that a significant fraction of the oocyst filtration is reversible and subject to time-dependent detachment.

Introduction

Cryptosporidium parvum, a protozoan parasite, is a primary etiologic agent of enterocolitis in mammals and potentially lethal for humans and animals who are immunosuppressed (*1*). The infectious stage of *C. parvum* is a protozoan oocyst. Unlike bacteria, the oocyst is biologically dormant, while outside its mammalian host and does not replicate and increase its numbers (*1*). However, the oocyst is shed in high concentrations (10^7/mL) with the feces of infected mammals. Consumption of as few as 10 oocysts can lead to infection. Epidemiological research in the United States and elsewhere encountered the oocyst in the feces of a wide variety of commonly occurring wild and domestic mammals (e.g., cattle, horses, ground squirrels, etc.). The presence of *C. parvum* is therefore not limited to environments directly impacted by human activity.

Two field surveys of *Cryptosporidium* spp. in groundwater, one study of 18 wells in Great Britain (*2*) and another more recent study of 463 groundwater samples from across the United States (*3*), indicate that contamination with low concentrations of *Cryptosporidium* is rather frequent. Evidence from transport studies in groundwater further suggests that colloids of a size similar to *C. parvum* (4.5−5.5 μm in diameter) may travel over significant distances (*4*). These experiments were conducted in coarse grained soils and aquifers, containing predominantly sands (grain size > 0.5 mm) and gravels, and in highly permeable fractured rocks. Protozoan cysts have also been reported to occur at a depth of 7 m in a confined shallow aquifer in Oklahoma, consisting of gravelly loamy sand (*5*). The only controlled laboratory studies relating to *C. parvum* transport in the subsurface were reported by Mawdsley et al. (*6*, *7*) who found significant subsurface transport of the oocyst in undisturbed soil columns and tilted soil boxes with clay loam, a silty loam, and a loamy sand soil. More recently, Brush (*8*) analyzed the surface runoff and leaching behavior of *C. parvum* in laboratory studies assuming that oocysts are subject to a simple advection-dispersion process and instantaneous, reversible sorption. These studies were limited to qualitative interpretation of *C. parvum* transport.

The purpose of our work is to develop a quantitative process-based understanding of the fate and transport of *C. parvum* that is relevant to oocyst transport at the laboratory and small field scale and that can be used to estimate *C. parvum* transport in porous media. The principal hurdle in empirically developing such understanding is the difficulty and cost of the analysis of *C. parvum* concentrations in porous media and water, which severely limits the number of experiments that can typically be implemented. Our approach is therefore two-pronged: First we review the known physical and chemical properties of *C. parvum* and formulate a hypothetical model of *C. parvum* transport. We then implement laboratory experiments to test the applicability of the theoretical model for various porous media under two different flow regimes. Results are compared to transport properties of other similarly sized colloids.

We postulate that oocysts enter the subsurface environment through a number of different pathways: (1) gravity dominated fluid movement in the fecal material deposited on the ground and direct infiltration into the unsaturated or saturated subsurface underlying the fecal matrix, (2) infiltration of contaminated surface runoff into the subsurface at some distance from the point of fecal discharge, and (3) infiltration of contaminated water from rivers, streams, and other surface waterbodies. The subsurface oocyst pathway may encompass one or several hydrologic regimes (unsaturated/saturated flow, fractured/porous media) in either spatial and/or temporal series. For drinking water protection we are primarily interested in those pathways that lead to springs, wells, or surface streams. We therefore focus on transport in saturated flow through porous (nonfractured) media.

Theory

Based on its size, the *C. parvum* oocyst is physically classified as a biological colloid. It has an almost spherical shape with a diameter of 4.5−5.5 μm (*9*). It is only slightly heavier than water with a density of 1.025−1.070 g/cm^3 (*9*). Surface charges measured by the ζ potential of the oocysts have been found to be neutral to slightly negative in most natural waters. Exact values depend on analytical methods used (*10*, *11*). Transport

* Corresponding author phone: (559)646-6500; fax: (559)646-6593; e-mail: thharter@ucdavis.edu.

† Present address: Geologisches Institut der Albert-Ludwigs-Universät, Albertstrasse 23b, D-79104 Freiburg, Germany.

10.1021/es990132w CCC: $19.00
Published on Web 11/18/1999

and filtration of such colloids in porous media is by advection, hydrodynamic dispersion, and interactive processes between colloids and solids surfaces (cf., refs *12* and *13*). A simple one-dimensional transport model in a steady-state flow field is

$$\frac{\partial c}{\partial t} + \frac{\rho_b \partial s}{\theta \partial t} = \nu d \frac{\partial^2 c}{\partial x^2} - \nu \left(\frac{\partial c}{\partial x} + \lambda c \right) \quad (1)$$

where c is the concentration of *C. parvum* oocysts in suspension, s is the concentration of *C. parvum* oocysts adsorbed reversibly on solids surfaces, ρ_b is bulk density, θ is porosity, d is the hydrodynamic dispersivity coefficient, v is the advective pore velocity, and λ is the colloid filtration coefficient. It is commonly observed that v in eq 1 is larger for colloids than for water (velocity enhancement) (*14*). Note, that eq 1 accounts for permanent deposition (filtration) of colloids through the first-order term $v\lambda c$ as well as for reversible deposition (sorption) through the second term on the left-hand side.

Several models have been introduced to describe the permanent removal of colloids by filtration onto the solid phase (*13, 15*). Mass balance considerations for the deposition of colloids in a clean packed filter bed of uniform spheres yield the following relationship between the filtration coefficient and the physical properties of filter bed and colloid (*15, 16*)

$$\lambda = \frac{3(1-\theta)}{2 d_c} \alpha \eta \quad (2)$$

where d_c is the median grain size diameter, α is an empirical constant referred to as collision efficiency, and η is the collector efficiency. Collector efficiency, η, represents attachment to solid surfaces due to colloid advection and diffusion, interception, buoyancy, and London−van der Waals attractive forces. These four characteristics are expressed in dimensionless form by the Peclet number, N_{Pe}, the interception number, N_R, the gravitation number, N_G, and the London−van der Waals constant, N_{Lo} (*15*) (Supporting Information, Supplement 1). In addition, a correction factor, A_s, is introduced that accounts for the pore geometry and its impact on packed bed collector efficiency. Rajagopalan and Tien showed that η is then computed from (*15, 16*, also see Supporting Information, Supplement 1)

$$\eta = 4A_s N_{Pe}^{-2/3} + A_s N_{Lo} N_R^{15/8} + 0.00338 A_s N_G N_R^{-0.4} \quad (3)$$

For the evaluation of the *C. parvum* transport behavior in column experiments, the collector efficiency, eq 3, can be computed a priori from the physical properties of the pore space (porosity, median grain size, bulk density), from the physical properties of water (density, viscosity, pore velocity), and from the physical properties of the colloid (density, mean diameter, particle diffusion coefficient, Supporting Information, Supplement 1). The collision efficiency, α, represents an empirical constant to account for the fact that repulsive forces at the collector surface (double-layer repulsion), which are not accounted for in eq 3, will prevent a fraction of the colloids from attachment (*13, 16*).

The reversible attachment of colloids can be treated equivalent to a sorption−desorption process. Reversible, instantaneous linear adsorption, first-order rate-limited adsorption−desorption, saturation-limited sorption models, or a combination of these have successfully been applied to the transport of biocolloids, such as viruses and bacteria (e.g., refs *12* and *17*). The instantaneous, linear sorption model or retardation model assumes that

$$s = K_d c \quad (4)$$

where K_d is the partitioning coefficient. Writing $R = 1 + \rho_b K_d / \theta$, where R is called the retardation coefficient, eqs 1 and 4 are combined to a single equation

$$R \frac{\partial c}{\partial t} = \nu d \frac{\partial^2 c}{\partial x^2} - \nu \left(\frac{\partial c}{\partial x} + \lambda c \right) \quad (5)$$

The first order, rate-limited adsorption−desorption process is defined by a forward sorption rate, k_f, and reverse sorption rate, k_r:

$$\frac{\partial s}{\partial t} = k_f c - k_r s \quad (6)$$

It can be shown that eq 1 with eq 6 is mathematically identical to the time-dependent colloid detachment model with exponentially decreasing detachment probability (*17*). Rate-limited sorption, eq 6, or time-dependent colloid detachment lead to significant asymmetry and tailing in the breakthrough curve.

For a continuous, steady injection with concentration c_0 into a column of length L, the steady-state outflow concentration, c, governed by eq 1 with $\partial c / \partial t = 0$ (and no reversible deposition) is determined by

$$\frac{c}{c_0} = \exp(-\lambda L) = \exp\left(-\frac{3}{2} \frac{(1-\theta)}{d_c} \alpha \eta L \right) \quad (7)$$

For transient transport conditions, analytical solutions to eq 1 exist for a number of boundary conditions (*18*). The following experiments are implemented to determine, whether saturated porous transport of *C. parvum* is consistent with the principles of colloid transport, eqs 1−3, and whether it is subject to ideal reversible sorption, eq 5, or nonideal reversible sorption, eq 6. Specifically, we empirically determine the degree of velocity enhancement (ratio of *C. parvum* velocity to water velocity), the magnitude of α, and the magnitude of the sorption parameters, where applicable.

Materials and Methods

General Approach. Five experiments were implemented in two replicate columns. The five experiments encompassed combinations of three different sands (fine, medium, coarse) and two pore velocities: a low pore velocity representative for groundwater velocities in sandy aquifers and a high pore velocity representative for short duration saturated soil infiltration rates during storm events.

Collection and Purification of *C. parvum* Oocysts. Fecal samples were collected per rectum from calves on two dairies in Tulare County, CA. Fecal samples containing *C. parvum* oocysts were washed through a series of 40, 100, 200, and 270 mesh sieves. Distilled water with 0.2% (w/v) Tween 20 (Tween water) was used as the wash diluent. The fecal suspension was placed in a graduated cylinder, and the larger particulate matter was allowed to settle out over 30 min. The resulting suspension was decanted off and centrifuged at 1000*g* for 10 min. Supernatant was discarded, and the pellet was resuspended in Tween water, centrifuged 10 min at 1000*g*, and supernatant discarded. The final fecal pellet was resuspended in Tween water to a final volume of 50−80 mL, depending on the size of the pellet.

A discontinuous sucrose gradient was used for purification of *C. parvum* oocysts (*19*). Final concentration of purified oocysts was determined by using a Bright Line Phase hemacytometer and then adjusted to achieve 1×10^7 oocysts per mL of stock solution which then was diluted to the desired concentration for the column experiments.

Column Experiments. Sand for the column fillings was collected at a gravel pit outcrop of a local alluvial aquifer in Fresno County, CA, and sieved to obtain three sand fractions ("coarse sand": 1.4−2.4 mm; "medium sand": 0.42−0.5 mm; "fine sand": 0.18−0.25 mm). The sand fractions were ultrasonically acid-cleaned, rinsed twice, and oven-dried at 70−80 °C. Clear acrylic columns (10 cm long, 5.1 cm in diameter) were wet-packed firmly and saturated with degassed tap water (DTW). Once the desired flow rate was established with a peristaltic pump, the following sequence of solutions was injected: 10 pore volumes (p.v.) DTW, 2.5 p.v. NaCl − tap water solution (electric conductivity (EC): 400 μS/cm), 10 p.v. DTW, 2.5 p.v. *C. parvum* solution (1×10^5 oocysts per mL), at least 5 and up to 250 p.v. DTW. A constant, uninterrupted flow velocity was maintained throughout the experiment. Oocyst input concentrations used in our experiment were similar to those observed in overland flow near infected fecal material (*20, 21*). Outflow was continuously collected in 10 mL aliquots for determination of EC and *C. parvum*. After completion of the experiment, the column filling was destructively sampled to obtain the *C. parvum* profile within the sand columns. All experiments were implemented in dual replicates. DTW is untreated (nonchlorinated), boiled local groundwater with an electric conductivity of 220 μS/cm and a pH of 7.9. The groundwater is a calcium−magnesium−sodium bicarbonate water with an ionic strength of 3×10^{-3} (Supporting Information, Supplement 2). Experiments were conducted at 23 °C.

Determining the Concentration of *C. parvum* Oocysts in Aliquots of Column Water. One hundred ten microliters of Tween 80 were added to each column water sample, resulting in a 0.1% Tween 80 solution. Samples were centrifuged for 15 min at 1000*g*, the supernatant was discarded, and the pellet was resuspended in 0.1% Tween water. Ten microliters of suspension was smeared onto a commercially prepared glass slide and air-dried overnight, and the direct immunofluorescent assay was performed according to the manufacturer's instructions (MERIFLUOR *Cryptosporidium/Giardia* direct immunofluorescent detection kit, Meridian Diagnostics, Inc., Cincinnati, OH). A negative and positive control was included for each set of slides. The total number of oocysts was enumerated for each sample, and the concentration of oocysts for each water sample was determined by adjusting for the estimated percent recovery of the immunofluorescent assay.

Determining the Concentration of *C. parvum* Oocysts in Column Sand. Fifteen grams of sample was measured into a 50 mL centrifuge tube. Extraction solution (ES) [1000 mL of 50 mM MOPS buffer, 5 mL of Tween 80 (0.5% v/v), 1 g of SDS (0.1% w/v)] was added to a final total volume of 35 mL. Three millimeter glass beads were added, and tubes were mixed for 30 min on a wrist action shaker. Supernatant was decanted into a 50 mL tube, 15 mL of ES was added to the grains, and the mixture was agitated with a pipet before the supernatant was again decanted into a 50 mL tube. Grains were rinsed three times as described above. All supernatants were combined in one tube, and the volume was adjusted to obtain the desired concentrations of oocysts. Representative 10 μL aliquots of these concentrates were pipetted and smeared onto a commercially prepared glass slide (MERIFLOUR), and the direct immunofluorescent assay was performed as before.

Parameter Calculation. Average pore water velocity, v_{cl}, and hydrodynamic dispersivity, d, in each column experiment were determined by fitting the measured breakthrough curve (BTC) of chloride to a one-dimensional analytical solution of the nonreactive advection-dispersion eq 5 with $R = 1$ and $\lambda = 0$ (*18*). Since the experiment was conducted by injecting tracer (and later oocysts) over a relatively long period (2.5 p.v.), the breakthrough curve had two main branches: one at the tracer front and one at the freshwater front. For each replicate, velocity and dispersivity was therefore determined twice to yield higher accuracy.

Velocity enhancement and filtration coefficient of the *C. parvum* oocysts are determined by calibrating v_{oo} (effective pore velocity of the oocysts) and λ such that the transient solution to eq 5 (clean-bed filtration) best matches the measured BTC of *C. parvum* (*18*). Alternatively, the filtration coefficient can be determined from eq 7 using the observed maximum concentration, c_{max}/c_0, during the quasi steady-state portion of the main BTC. We also measured the total mass eluted during the column experiments ($t \leq 5$ p.v.). The total mass eluted divided by the total mass injected is called the fractional penetration, F_p (*22*). It is identical to c_{max}/c_0 if nonequilibrium sorption is small. It can also be used *in lieu* of c_{max}/c_0 to calculate λ. Independent from the BTC, λ can also be determined by measuring $-\partial(\ln s)/\partial x$ in the column profile after completion of the experiment (Supporting Information, Supplement 3).

The kinetic sorption parameters, k_f and k_r, are obtained by calibrating v_{oo}, λ, k_f, and k_r in the one-dimensional transient solution to eqs 1 and 6 (filtration with detachment) to the measured oocyst BTC (*18*). For calibration of all oocyst BTCs, d is known from the respective chloride tracer experiment. After the calibration is implemented, velocity enhancement is computed as $(v_{oo}/v_{cl} - 1)$. The collision efficiency, α, is obtained by solving eq 2 for α using the calibrated λ value and the η value computed from the physical properties of each experiment (eq 3). For the determination of η, the collector diameter, d_c, must be approximated by a characteristic diameter of the sand medium. It was shown for the filtration of *E. coli* (length: 2−3 μm) and of *Pseudomonas fluorescens* (approximate length: 1 μm) in glass beads and various quartz sands that the collector diameter is characterized by the size of the smaller particles in the filterpack (*23, 24*). Therefore, we approximated d_c by the lower limit of the fine, medium, and coarse sand grain size range, respectively. Mean oocyst diameter, d_p, is 5 μm; mean oocyst density is 1050 kg m^{-3} (*9*). The effective porosity, θ, for oocyst transport is computed from the ratio of applied flow rate, U (also called Darcy velocity, superficial velocity, or approach velocity), to oocyst pore velocity, v_{oo}.

Results and Discussion

The applied flow rate for the "fast" experiments" is 7.1 m/d. For the "slow" experiment it is 0.71 m/d. Calibrated pore water velocities, v_{cl}, vary from 14.1 to 15.1 m/d in the fast experiments and from 1.41 to 1.42 m/d for the slow experiments. Effective porosities for chloride transport, U/v_{cl}, range from 48% to 51% in the fast experiments and are 50% for the slow experiments. The dispersivities, d, of the coarse, medium, and fine sands are 5, 1, and 0.3 mm, respectively.

The total *C. parvum* recovery in the experiments (oocysts eluted plus oocysts recovered from the column profile) range from 41% to 93% (Table 1). No statistically significant differences are observed between the two replicate BTCs of each experiment. Neither are significant differences observed between parameters describing the tracer front and those describing the freshwater front. The observed recovery rate and eluent oocyst variability (Figure 1) are consistent with similar microbial column studies on, e.g., *C. parvum* oocysts (*8*), *E. coli* bacteria (*23, 26*), 1 μm polystyrene beads (*23, 26*), and *Pseudomonas fluorescens* bacteria (*22*). Figure 2 shows measured and fitted *C. parvum* BTCs on a log-concentration scale to emphasize the observed nonideal sorption (detachment) behavior. Corresponding parameters are listed in Table 1. Column profiles of *C. parvum* concentration on the sand media after completion of the experiment are shown in Figure 3.

TABLE 1: Chloride and Oocyst Velocity, Effective Porosity, Velocity Enhancement, Steady-State Concentration, and Mass Retained in the Soil Column for Each Experiment[a]

	CS fast	CS slow	MS fast	MS slow	FS fast
chloride pore velocity, v_{cl} [m/d]	14.2	1.41	14.8	1.41	14.1
chloride effective porosity [%]	50	50	48	50	51
oocyst pore velocity, v_{oo} [m/d]	16.8	1.94	16.1	1.57	14.1
oocyst effective porosity [%]	42	37	44	45	51
velocity enhancement [%]	19	37	9	11	0
fitted BTC: c_{max}/c_0 [%]	74	10	20	0.22	0.52
mass eluted: F_p [%]	69	10	14	0.23	0.7
mass retained [%]	15	40	73	74	40
% total recovery	84	50	87	74	41
filtration rate, λ [m^{-1}]	3.0	23	16	61	53
collision efficiency, α	0.95	0.37	1.1	0.69	0.85

[a] The relative total recovery is the sum percent mass eluted plus percent mass retained in the column. The filtration rate is computed by using c_{max}/c_0 from the fitted BTC. CS: coarse sand, MS: medium sand, FS: fine sand, fast: high flow rate, slow: low flow rate.

Initial Arrival and Advective Velocity of *C. parvum*: Velocity Enhancement. The initial arrival of *C. parvum* in all replicates of each experiment is earlier than that of chloride. Due to the small dispersivity, *C. parvum* concentrations can be as high as 20% before any significant (≥5%) changes in chloride concentrations occur. Velocity enhancement is consistently observed in both the increasing and the decreasing branch of the breakthrough curves. Velocity enhancement is less pronounced at higher velocity and smaller grain size (Table 1). In the fast fine sand experiment the calibrated v_{oo} value shows no velocity enhancement. However, in the earliest part of that BTC, significant oocyst concentrations are observed before any increase occurs in the chloride concentration (Figure 1).

Velocity enhancement of *C. parvum* is in principle consistent with our understanding of colloid transport (*14*), where it is also referred to as hydrodynamic chromatography (*27*). The transport velocity of colloids is higher than that of water because not all pores are accessible for the colloids (inaccessible pore volume) and colloids are excluded from the margins of the pore throats (excluded pore volume). In coarse grained porous media, the latter is the dominant cause of velocity enhancement (*28*). Observed effective porosities for oocyst transport are therefore smaller than those observed for chloride transport and range from 37% to 51% (Table 1).

In contrast to our findings, Small (*27*) determined that the enhancement increases as the mean grain size of the packing bed decreased. However, filtration coefficients in Small's experiments (<1 m^{-1}) were much lower than those observed here (3−61 m^{-1}, see below). Higgo et al. (*29*) showed that velocity enhancement was largest for particles with very small filtration coefficients (<1 m^{-1}). Only small enhancement was found for transport of 0.1 μm beads in sieved sand (125−250 μm fraction), where the filtration coefficient was shown to be in the range of 35−56 m^{-1}. Flagellated protozoa and microspheres did not exhibit significant velocity enhancement traveling in a sandy aquifer with moderate heterogeneity over distances of 1−3.6 m (*4*). The velocity enhancement observed in our experiments may therefore disappear for larger travel distances.

It is often found that low ionic strength increases velocity enhancement due to the expansion of the electrical double layer at the solids surface (*27*). For 0.21 μm polysterene beads in 145 μm Entraigues sand (λ < 1), for example, velocity enhancement was significant when ionic strength was 10^{-3} or less (*30*). Experiments by Jewett et al. (*22*) demonstrated that increased ionic strength not only decreases velocity enhancement but also the fractional penetration, F_p. Lower fractional penetration (i.e., higher filtration, λ) was accompanied by less velocity enhancement. This latter observation is consistent with our results, which show that in fine sands the enhancement effect on *C. parvum* is masked by the high clean bed filtration capacity of the sand column (k_c > 20 m^{-1}). However, in the medium and coarse sand experiments, the ionic strength in our experiment is high enough to keep double-layer thickness small relative to the pore size (see next section). Velocity enhancement is therefore primarily due to pore size exclusion and pore inaccessibility.

Filtration and Collision Efficiency of *C. parvum*. As expected from filtration theory, maximum eluent concentration, and fractional penetration of *C. parvum* decrease with smaller grain size and lower pore velocity (Table 1) leading to the largest residual concentrations in the slow medium sand (MS slow) and fast fine sand (FS fast) experiments. The filtration coefficients (computed by calibration to the measured BTC) range from 3 m^{-1} in the fast coarse sand (CS fast) experiment to 61 and 53 m^{-1} in the MS slow and FS fast experiments, respectively. The concentration profiles in all but the fast coarse sand (CS fast) column show the largest concentration of oocysts near the top (inflow boundary) of the sand column (Figure 3). Similar to outflow concentrations, sorbed concentrations in the profile decrease exponentially with distance from the inflow boundary (Supporting Information, Supplement 3). Semilogarithmic concentration profiles for "CS slow", "MS fast" (without value at $z = 0.1$ m), "MS slow" (without value at $z = 0.1$ m), and "FS fast" are approximately linear with negative slopes of 20, 19, 29, and 35 m^{-1}, respectively. As expected from the clean-bed filtration model (Supporting Information, Supplement 3), these values approximately match the filtration coefficients that are obtained from the BTC at $L = 10$ cm (Table 1). Least agreement is observed for MS slow and FS fast.

The measured collision efficiencies, α, range from 0.37 to 1.1 (Table 1), which is near or slightly above the theoretical limit of complete efficiency, $\alpha = 1$, indicating that repulsive double layer forces are generally weak. Large values of α are also found by applying the proposed filtration model to the *C. parvum* transport experiments reported by Brush (*8*). Using their data in our eqs 2, 3, and 7, we calculate the collision efficiencies, α. They are 1.6 and 0.53 in 2000 μm glass bead and 850 μm sand packing, respectively. The high α values are consistent with the low but significant ionic strength of the groundwater used in the experiments and the known neutral to only slightly negative ζ potentials characterizing oocyst surface charges (*10, 11*). For example, in experiments with 1 μm polystyrene particles (density: 1050 kg m^{-3},

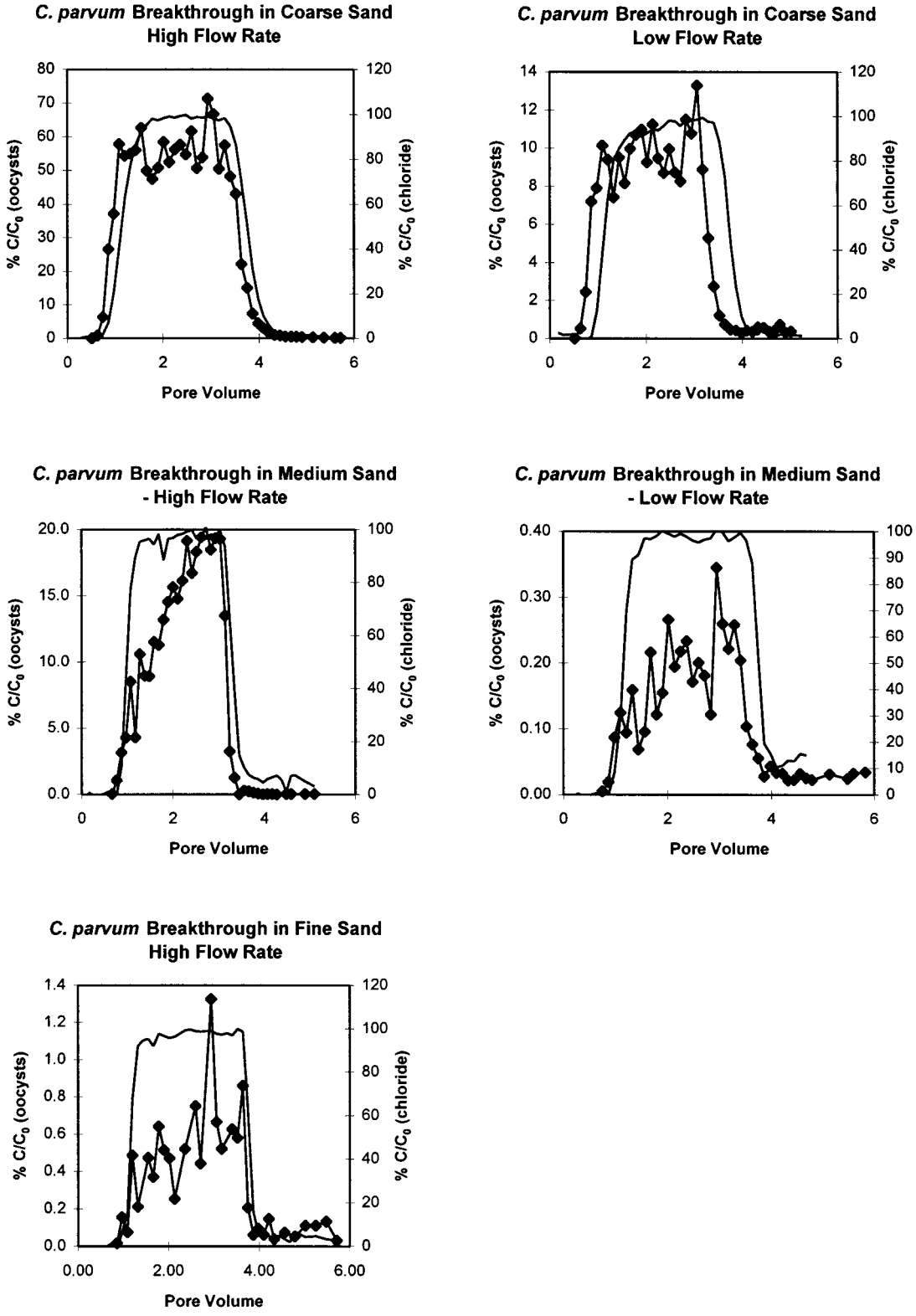

FIGURE 1. Measured *C. parvum* (diamonds) and chloride (line) breakthrough curves.

electrolyte: Ca−Mg−Cl−SO_4 water, negative ζ potential due to carboxyl groups at the particle surface), Matthess et al. (*23*) empirically derived the following correlation between α and ionic strength

$$\alpha = -1.56 + 0.355 \ln\left(\frac{\chi}{\chi_0}\right) \qquad (8)$$

where $\chi_0 = 1\ \text{nm}^{-1}$ and χ is the Debye−Hückel parameter, which is a function of the ionic strength, I, and is inversely related to the thickness of the double layer (*23*). The influence of ionic strength on α was found to vanish at ionic strengths significantly above 0.001 M. In experiments on *Pseudomonas fluorescens* P17 drastic decreases in collision efficiency occurred only below ionic strengths of 10^{-3}−10^{-2} (*22*). For the groundwater used in our experiments ($I = 0.003$ M), $1/\chi$ is only 8 nm. The collision efficiency for *C. parvum* oocysts predicted by eq 8 is therefore 0.86. The agreement between

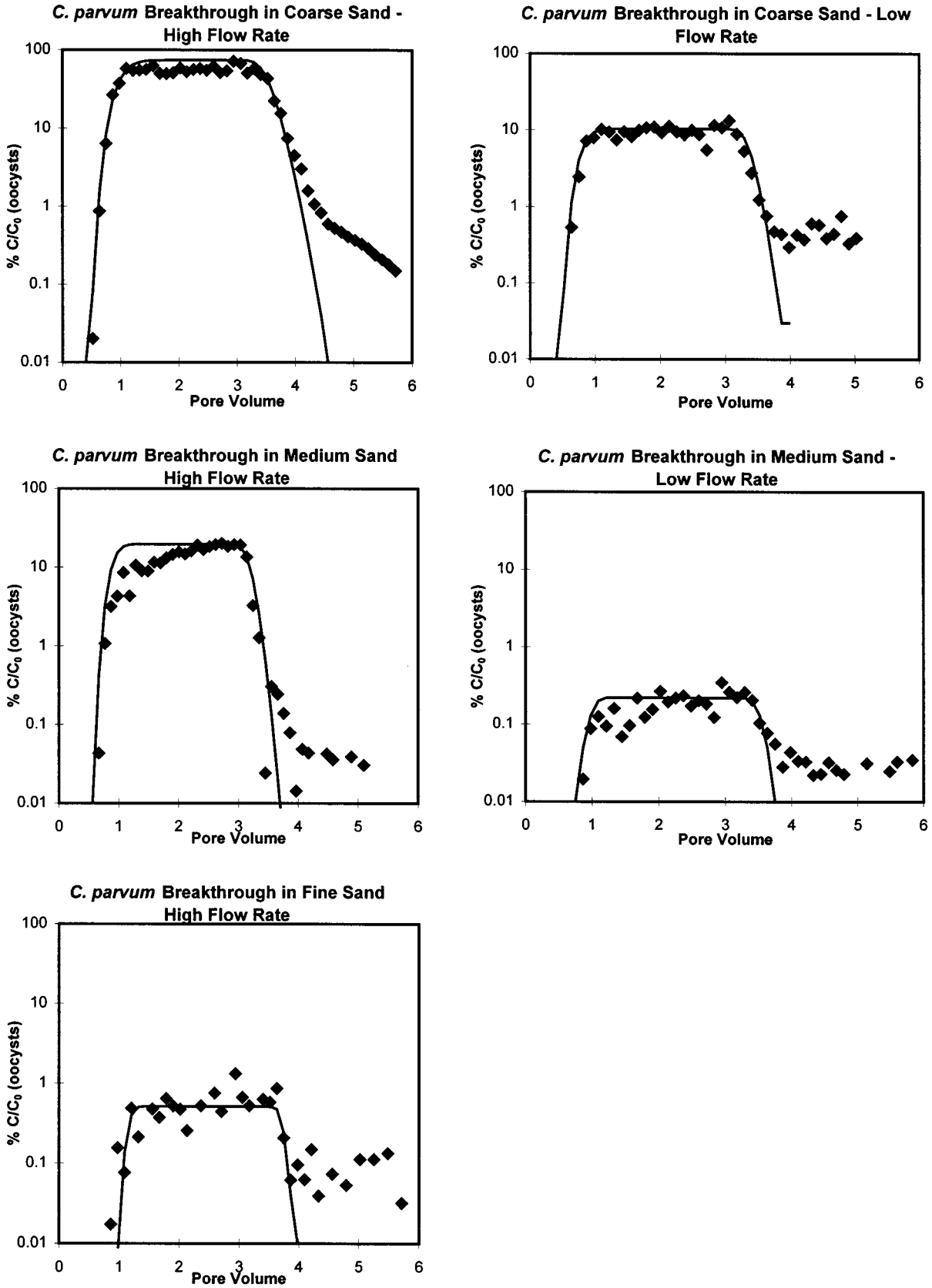

FIGURE 2. Measured (diamonds) and modeled (line) *C. parvum* breakthrough curves on a log concentration scale. Here, the model, eqs 1−3, accounts for filtration by deposition and assumes that no reversible sorption takes place ($\partial s/\partial t = 0$).

our measured α values (0.37−1.1) for *C. parvum* and that predicted by eq 8 (0.86) is comparable to the agreement found between measured and predicted values for *E. coli* (length: 2−3 μm) (*23, 26*). Note, that eq 8 does not explicitly account for the surface charge (ζ potential) of the colloid. The ζ potential of *C. parvum* oocysts is less negative than that of the polystyrene particles for which eq 8 was developed, i.e., interaction between the oocyst and the double layer is less

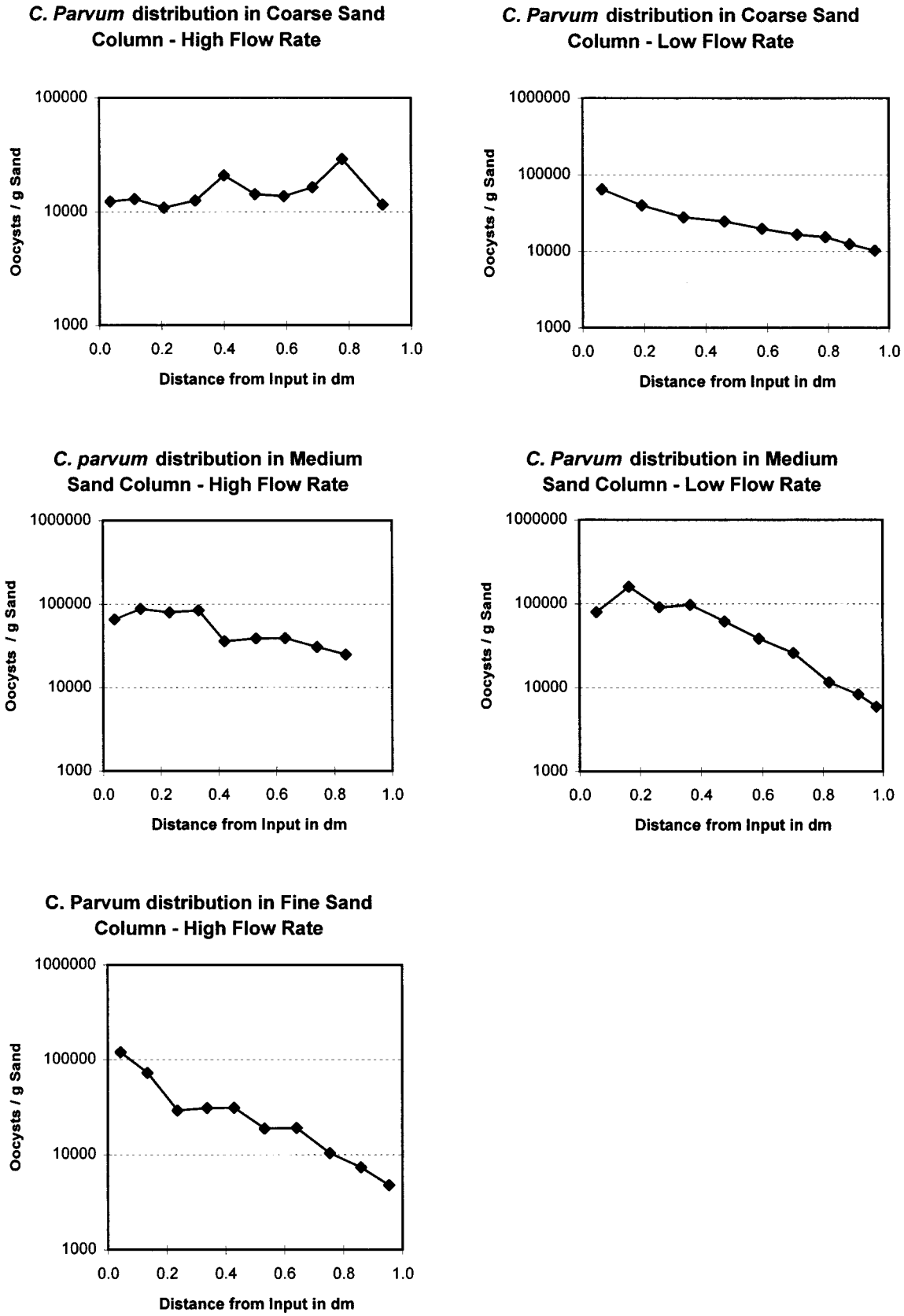

FIGURE 3. Column profiles of *C. parvum* after the completion of the experiment.

than between the polystyrene particles and the double layer. A significant decrease in collision efficiency should therefore not be expected unless ionic strength is much less than 10^{-3}.

Differences between the idealized model of filtration theory, eq 3, and the actual porous medium in the experiments may potentially contribute to the high collision efficiencies. For example, the experiments were implemented with river sands that are partially reworked sediments of granitic origin, poorly rounded with numerous edges, and high amounts of platelike mica. Although porosity is high,

TABLE 2: Parameter Sensitivity Analysis of the Collision Efficiency α to Measured Parameters[a]

sensitivity parameter	CS fast	CS slow	MS fast	MS slow	FS fast
c_{max} * 1.1	0.81	0.35	1.04	0.68	0.83
c_{max} * 0.9	1.28	0.38	1.17	0.71	0.87
$d_p = 5.5\ \mu$m, $\rho_b = 1070$ kg/m^3	0.60	0.21	0.87	0.45	0.74
$d_p = 4.5\ \mu$m, $\rho_b = 1025$ kg/m^3	1.74	0.89	1.41	1.22	0.98
$\theta + 2\%$	1.08	0.43	1.25	0.79	0.96
$\theta - 2\%$	0.83	0.31	0.97	0.61	0.75

[a] The table gives the α values computed via ref *7* after recomputing η for each of the five experiments. The first column describes the change in input parameter(s) for the η and α computation. Only one or two parameters were changed at a time; all others were kept at the value given in the text.

dead end pores and planar contact of grain surfaces resulting from high angularity of grains may lead to localized straining not accounted for by filtration theory. Angularity and rough surfaces also enhance the effect of charge heterogeneity on the surface of the sand grains. Both, surface roughness and charge heterogeneity enhance the filtration capacity of sand grains [e.g., refs *13* and *26*]. Increased attachment to heterogeneous charge surfaces that attract negatively charged oocysts is consistent with the observation of high α values and reversible attachment (sorption, see below).

Measurement errors may also contribute to the range of α values observed in the experiments. A sensitivity analysis of α with respect to several measured properties is shown in Table 2. The calculated values of α for the CS and MS experiments are sensitive in particular to oocyst density and oocyst diameter. If we assume that both the density and the diameter of the oocysts are equal to the 90th percentile of the size/density distribution empirically determined by Medema et al. (*9*), the range of α values decreases by approximately one-third. On the other hand, assuming values equal to the 10th percentile of the size/density distribution increases α values by as much as a factor 2. The estimated α values are also sensitive to the effective porosity estimates (accuracy: ±5%) and maximum eluent concentration (accuracy: ±10%) (Table 2).

We observe a peculiar dependence between α and pore velocity not explained by the theoretical model: α significantly decreases with decreasing pore velocity. While the small number of experiments does not allow statistical extrapolation, the same observation is made in dozens of experiments with *E. coli*, *Pseudomonas cepacia*, and *Streptococcus faecalis* (*23, 26*) (effective grain size: 190−5300 μm, pore velocity: 0.75−7.5 m/d, similar to that in our experiments). For all three bacteria, the reported ratio of measured λ to predicted λ, which is equivalent to our α, is smallest at the low pore velocity and increases with larger pore velocities. Although the experimental results are variable, the trend is significant for all three bacteria (*21*, Figure 4.5−4.7). These findings indicate either that the collector efficiency η does not sufficiently capture velocity dependent filtration phenomena or that chemical interactions between collector and biocolloid (represented by α) are indeed velocity dependent.

We conclude that observed *C. parvum* filtration and collision efficiencies are consistent with our general understanding of colloid transport in porous media. The empirical eq 8 provides good estimates of *C. parvum* collision efficiencies. Most importantly, our experiments show that the *C. parvum* concentration in the main breakthrough curve and oocyst retention in the sand column are well predicted by colloid filtration theory. Equation 5 (with R ranging from 0.9 to 1 to reflect velocity enhancement) and eqs 2 and 3 (with collision efficiencies ranging from 0.5 to 1) should

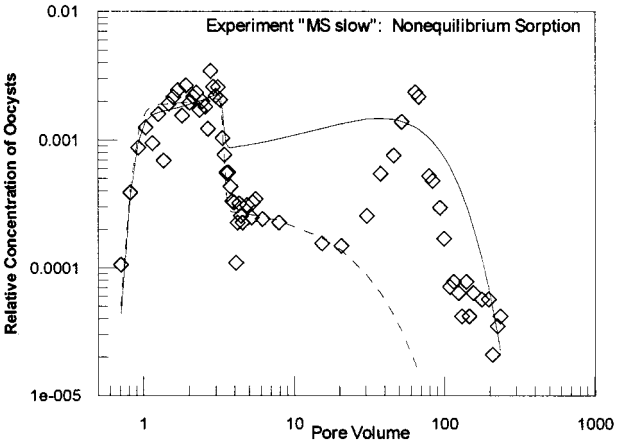

FIGURE 4. Measured (diamonds) and fitted breakthrough curves for *C. parvum* in the MS slow experiment. Parameters for the solid/dashed line models, respectively: k_c = 28/56 m^{-1}, k_r = 6.5E−04/7.8E−04 min^{-1}, k_f = 0.014/0.0036 min^{-1}.

therefore provide a useful tool to predict *C. parvum* transport in saturated sandy porous media. On the other hand, based on these theoretical considerations, transport of oocysts in clay, silt, and very fine sand sediments must be subject to rapid filtration and straining unless macropores, fractures, or other inhomogeneities provide alternative pathways as shown empirically by Mawdsley et al. (*6, 7*).

Remobilization of *C. parvum* After Initial Clean Bed Filtration: Nonideal Transport. The clean-bed filtration model, eq 3, has been specifically developed for the initial filtration of particles on clean beds. It does not account for saturation of surface sites or the later detachment of colloids. In our experiments, we observe significant tailing in the late part of the BTC when compared to the model predictions, eq 5 (solid line, Figure 2). The MS slow experiment was continued by flushing the sand column with 250 p.v. of DTW. Measurable concentrations of oocysts were observed throughout the duration of the experiment in both replicates (one replicate was terminated after approximately 60 p.v. for analysis of profile concentrations). A secondary concentration peak appears with a large retardation factor, $R = k_f/k_r = 68$ (Figure 4). The secondary breakthrough concentration peaked at 0.25% compared to 0.30% during the first breakthrough. The second peak, which is subject to much less apparent variability than the primary breakthrough curve, shows significant late time tailing. In the oocyst BTCs of all but the coarse sand experiments, we also observe significant skewness in the initial breakthrough such that the maximum eluent concentration is not attained until approximately 3 p.v., while the theoretical model predicts a symmetric BTC (Figure 2). The negative slope of the log concentration of oocysts retained in the sand columns of the MS slow and FS fast experiment is also significantly smaller than expected from filtration theory (see above).

In the case of *C. parvum*, it therefore appears that a significant amount of oocysts are remobilized after being initially filtered. Remobilization leads to the nonideal transport tailing observed in the experiments (Figure 2) and decreased slope in the log residual concentrations of the column profile. In a parsimonious mathematical model that combines first-order filtration and first-order kinetic sorption, eqs 1 and 6, colloids in solution are subject to either one of two processes: irreversible sorption through filtration, represented by the sink term $v\lambda c$; and reversible, nonequilibrium sorption, represented by the first-order kinetic source term $\partial s/\partial t$. While the first-order kinetic model only partially explains the observed behavior (Figure 4), it reproduces the observed skewness in the initial breakthrough, the tailing in

the later BTC, and the peculiar double-peak behavior observed in MS slow (Figure 4). Double peaks with similar peak concentrations (as observed here) develop only within a very narrow magnitude range for sorption rates, k_f and k_r, giving relatively high confidence to the calibrated values of k_f and k_r. The calibrated filtration rate in the reversible sorption model (Figure 4) is 28 m^{-1} compared to 61 m^{-1} obtained by calibration of the initial BTC to eq 5 (Table 1). Hence, half of all attachment events appear to be reversible. The measured oocyst mass eluted between 5 and 250 p.v. is 3.3% of the input mass. This is a significant increase in measured fractional penetration, F_p, from 0.2% at 5 p.v. to 3.5% at 250 p.v.

The simple first-order kinetic sorption/filtration model qualitatively demonstrates that kinetically controlled attachment/detachment processes control the long-term transport of *C. parvum* oocysts. However, the modeled peak is not nearly as distinctive as in the experiment. The model also shows a relatively steep decline in concentrations after 100 p.v., while continued tailing occurs in the experiment. Further experimental and theoretical research is needed to measure and explain the long-term elution behavior of *C. parvum*. Such work will be particularly important for our understanding of the long-term fate of the oocysts in the subsurface. We conclude that the clean bed filtration model without detachment provides an excellent tool to predict maximum oocyst concentrations following a *C. parvum* contamination event. After the initial breakthrough, however, contaminated porous media itself becomes a significant source of oocysts potentially leading to long-term, low-level elution of *C. parvum* oocysts.

Acknowledgments

This work has been funded, in parts, by the Studienstiftung des Deutschen Volkes and by a University of California competitive research grant. We acknowledge the thorough and helpful comments provided by the anonymous reviewers. We also thank David Jewett, Bruce Logan, Charles Brush, Ron Harvey, and Tim Ginn for their generous advice.

Supporting Information Available

Supplement 1 contains a detailed explanation of the parameters in eq 4 and how they are computed. Supplement 2 is a chemical analysis of the major ions in the DTW. Supplement 3 is a derivation of the formula used to determine λ from the slope of the oocyst concentration profile in the sand columns.

Literature Cited

(1) Casemore, D. P.; Wright, S. E.; Coop, R. L. In *Cryptosporidium and Cryptosporidiosis*; Fayer, R., Ed.; CRC Press: Boca Raton, FL, 1997; p 65−92.
(2) Lisle, J. T.; Rose, J. B. *J. Water SRT − Aqua* **1995**, *44*(3), 103−117.
(3) Hancock, C. M.; Rose, J. B.; Callahan, M. Presentation for International Symposium on Waterborne *C. parvum*: Newport Beach, CA, March 1997.
(4) Harvey, R. W.; Kinner, N. E.; Bunn, A.; MacDonald, D.; Metge, D. *Appl. Environ. Microbiol.* **1995**, *61*(1), 209−217.
(5) Sinclair, J. L.; Ghiorse, W. C. *Appl. Environ. Microbiol.* **1987**, *53*(5), 1157−1163.
(6) Mawdsley, J. L.; Brooks, A. E.; Merry, R. J. *Biol. Fertil. Soils* **1996**, *21*, 30−36.
(7) Mawdsley, J. L.; Brooks, A. E.; Merry, R. J.; Pain, B. F. *Biol. Fertil. Soils* **1996**, *23*, 215−220.
(8) Brush, C. F. Ph.D. Dissertation, Cornell University: Ithaca, NY, 1997. 175 p.
(9) Medema, G. J.; Schets, F. M.; Teunis, P. F. M.; Havelaar, A. H. *Appl. Environ. Microbiol.* **1998**, *64*(11), 4460−4466.
(10) Brush, C. F.; Walter, M. F.; Anguish, L. J.; Ghiorse, W. C. *Appl. Environ. Microbiol.* **1998**, *64*(11), 4439−4445.
(11) Drozd, C.; Schwartzbrod, J. *Appl. Environ. Microbiol.* **1996**, *62*(4), 1227−1232.
(12) Harvey, R. W.; Garabedian, S. P. *Environ. Sci. Technol.* **1991**, *25*, 178−185.
(13) Ryan, J. N.; Elimelech, M. *Colloids Surfaces A: Physicochem. Eng. Aspects* **1996**, *107*, 1−56.
(14) DeMarsily, G. *Quantitative Hydrogeology*; Academic Press: San Diego, CA, 1986; 440 p.
(15) Logan, B. E.; Jewett, D. G.; Arnold, R. G.; Bouwer, E. J.; O'Melia, C. R. *J. Environ. Eng.* **1995**, *121*(12), 869−873.
(16) Rajagopalan, R., Tien, C. *AIChE J.* **1976**, *22*, *2*(3), 523−533.
(17) Johnson, W. P.; Blue, K. A.; Logan, B. E.; Arnold, R. G. *Water Resour. Res.* **1995**, *31*(11), 2649−2658.
(18) Toride, N.; Leij, F. J.; VanGenuchten, M. Th. *The CXTFIT Code for Estimating Transport Parameters form Laboratory or Field Tracer Experiments, Version 2.0*; U.S. Salinity Laboratory: Riverside, CA, 1995; 121 p.
(19) Arrowood, M. J.; Sterling, C. R. *J. Parasitology* **1987**, *73*, 314−319.
(20) Tate, K. W.; Atwill, E. R.; George, M. R.; McDougald, N. K.; Larsen. R. E. *J. Range Management* **1999**, in press.
(21) Atwill, E. R.; Tate, K. W.; George, M. R.; McDougald. N. K. *Proceedings: Symposium on Rangeland Management and Water Resources*; American Water Resources Association: Reno, NV, 1998; p 446.
(22) Jewett, D. G.; Hilbert, T. A.; Logan, B. E.; Arnold, R. G.; Bales, R. C. *Water Resources* **1995**, *29*(7), 1673−1680.
(23) Matthess G.; Bedbur, E.; Gundersmann, K.-O.; Loof, M.; Peters, D. *Zbl. Hyg.* **1991**, *191*, 347−395.
(24) Martin, M. J.; Logan, B. E.; Johnson, W. P.; Jewett, D. G.; Arnold, R. G. *J. Environ. Eng.* **1996**, *122*(5), 407−415.
(25) Yao, K.; Habibian, M. T.; O'Melia, C. R. *Environ. Sci. Technol.* **1971**, *5*(11), 1105−1112.
(26) Matthess, G.; Bedbur, E.; Gundersmann, K.-O.; Loof, M.; Peters, D. *Zbl. Hyg.* **1991**, *191*, 53−97.
(27) Small, H. *J. Colloid Interface Sci.* **1974**, *48*(1), 147−161.
(28) Sorbie, K. S. *Polymer-Improved Oil Recovery*; Blackie: Glasgow, 1991.
(29) Higgo, J. J. W.; Williams, G. M.; Harrison, I.; Warwick, P.; Gardiner, M. P. *Colloids Surfaces A.; Physicochem. Eng. Aspects* **1993**, *73*, 179−200.
(30) Harmand, B.; Sardin, M. In *Transport and Reactive Processes in Aquifers*; Dracos and Stauffer, Eds.; Balkema: Rotterdam, 1994; pp 149−154.

Received for review February 5, 1999. Revised manuscript received October 7, 1999. Accepted October 12, 1999.

ES990132W